

Figure 7.5 Standing normal shock.

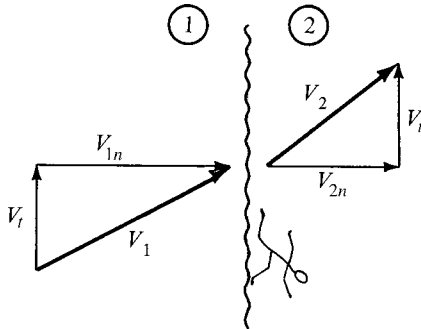


Figure 7.6 Standing normal shock plus tangential velocity.

We would normally view this picture in a slightly different manner. If we concentrate on the total velocity (rather than its components), we see the flow as illustrated in Figure 7.7 and immediately notice several things:

1. The shock is no longer normal to the approaching flow; hence it is called an *oblique shock*.
2. The flow has been deflected *away* from the normal.
3.  $V_1$  must still be supersonic.
4.  $V_2$  could be supersonic (if  $V_t$  is large enough).

We define the *shock angle*  $\theta$  as the acute angle between the approaching flow ( $V_1$ ) and the shock front. The *deflection angle*  $\delta$  is the angle through which the flow has been deflected.

Viewing the oblique shock in this way, as a combination of a normal shock and a tangential velocity, permits one to use the normal-shock equations and table to solve oblique-shock problems for perfect gases provided that proper care is taken.

$$V_{1n} = V_1 \sin \theta \tag{7.2}$$

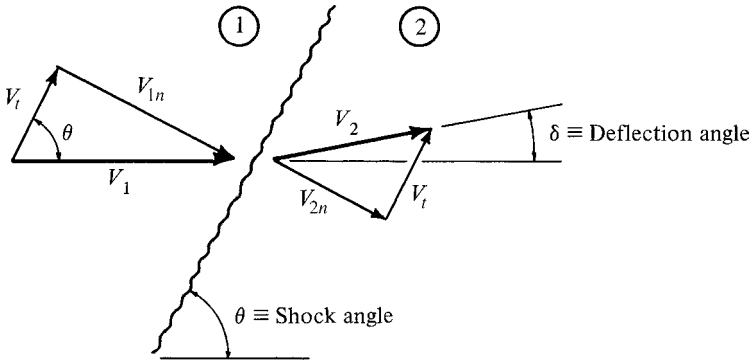


Figure 7.7 Oblique shock with angle definitions.

Since sonic velocity is a function of temperature only,

$$a_{1n} = a_1 \quad (7.3)$$

Dividing (7.2) by (7.3), we have

$$\frac{V_{1n}}{a_{1n}} = \frac{V_1 \sin \theta}{a_1} \quad (7.4)$$

or

$$M_{1n} = M_1 \sin \theta \quad (7.5)$$

Thus, if we know the approaching Mach number ( $M_1$ ) and the shock angle ( $\theta$ ), the normal-shock table can be utilized by using the *normal Mach number* ( $M_{1n}$ ). This procedure can be used to obtain *static* temperature and pressure changes across the shock, since these are unaltered by the superposition of  $V_t$  on the original normal-shock picture.

Let us now investigate the range of possible shock angles that may exist for a given Mach number. We know that for a shock to exist,

$$M_{1n} \geq 1 \quad (7.6)$$

Thus

$$M_1 \sin \theta \geq 1 \quad (7.7)$$

and the minimum  $\theta$  will occur when  $M_1 \sin \theta = 1$ , or

$$\theta_{\min} = \sin^{-1} \frac{1}{M_1} \tag{7.8}$$

Recall that this is the same expression that was developed for the Mach angle  $\mu$ . Hence *the Mach angle is the minimum possible shock angle*. Note that this is a limiting condition and really no shock exists since for this case,  $M_{1n} = 1.0$ . For this reason these are called *Mach waves* or *Mach lines* rather than shock waves. The *maximum* value that  $\theta$  can achieve is obviously  $90^\circ$ . This is another limiting condition and represents our familiar normal shock.

Notice that as the shock angle  $\theta$  decreases from  $90^\circ$  to the Mach angle  $\mu$ ,  $M_{1n}$  decreases from  $M_1$  to 1. Since the strength of a shock is dependent on the *normal* Mach number, we have the means to produce a shock of *any strength* equal to or less than the normal shock. Do you see any possible application of this information for the case of a converging–diverging nozzle with an operating pressure ratio someplace between the second and third critical points? We shall return to this thought in Section 7.8.

The following example is presented to provide a better understanding of the correlation between oblique and normal shocks.

**Example 7.3** With the information shown in Figure E7.3a, we proceed to compute the conditions following the shock.

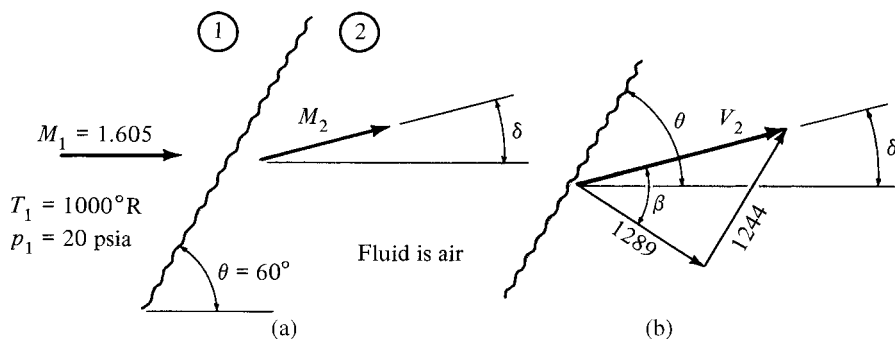


**Figure E7.3**

$$\begin{aligned}
 a_1 &= (\gamma g_c R T_1)^{1/2} = [(1.4)(32.2)(53.3)(1000)]^{1/2} = 1550 \text{ ft/sec} \\
 V_1 &= M_1 a_1 = (1.605)(1550) = 2488 \text{ ft/sec} \\
 M_{1n} &= M_1 \sin \theta = 1.605 \sin 60^\circ = 1.39 \\
 V_{1n} &= M_{1n} a_1 = (1.39)(1550) = 2155 \text{ ft/sec} \\
 V_t &= V_1 \cos \theta = 2488 \cos 60^\circ = 1244 \text{ ft/sec}
 \end{aligned}$$

Using information from the normal-shock table at  $M_{1n} = 1.39$ , we find that  $M_{2n} = 0.7440$ ,  $T_2/T_1 = 1.2483$ ,  $p_2/p_1 = 2.0875$ , and  $p_{t2}/p_{t1} = 0.9607$ . Remember that the static temperatures and pressures are the same whether we are talking about the normal shock or the oblique shock.

$$\begin{aligned}
 p_2 &= \frac{p_2}{p_1} p_1 &= (2.0875)(20) &= 41.7 \text{ psia} \\
 T_2 &= \frac{T_2}{T_1} T_1 &= (1.2483)(1000) &= 1248^\circ\text{R} \\
 a_2 &= (\gamma g_c R T_2)^{1/2} &= [(1.4)(32.2)(53.3)(1248)]^{1/2} &= 1732 \text{ ft/sec} \\
 V_{2n} &= M_{2n} a_2 &= (0.7440)(1732) &= 1289 \text{ ft/sec} \\
 V_{2t} &= V_{1t} &= V_i &= 1244 \text{ ft/sec} \\
 V_2 &= [(V_{2n})^2 + (V_{2t})^2]^{1/2} &= [(1289)^2 + (1244)^2]^{1/2} &= 1791 \text{ ft/sec} \\
 M_2 &= \frac{V_2}{a_2} &= \frac{1791}{1732} &= 1.034
 \end{aligned}$$

Note that although the *normal component* is subsonic after the shock, the velocity after the shock is supersonic in this case.

We now calculate the deflection angle (Figure E7.3b).

$$\begin{aligned}
 \tan \beta &= \frac{1244}{1289} = 0.9651 & \beta &= 44^\circ \\
 90 - \theta &= \beta - \delta
 \end{aligned}$$

Thus

$$\delta = \theta - 90 + \beta = 60 - 90 + 44 = 14^\circ$$

Once  $\delta$  is known, an alternative calculation for  $M_2$  would be

$$\boxed{M_2 = \frac{M_{2n}}{\sin(\theta - \delta)}} \quad (7.5a)$$

$$M_2 = \frac{0.7440}{\sin(60 - 14)} = 1.034$$

**Example 7.4** For the conditions in Example 7.3, compute the stagnation pressures and temperatures.

$$\begin{aligned}
 p_{t1} &= \frac{p_{t1}}{p_1} p_1 = \left( \frac{1}{0.2335} \right) (20) = 85.7 \text{ psia} \\
 p_{t2} &= \frac{p_{t2}}{p_2} p_2 = \left( \frac{1}{0.5075} \right) (41.7) = 82.2 \text{ psia}
 \end{aligned}$$

If we looked at the normal-shock problem and computed stagnation pressures on the basis of the *normal* Mach numbers, we would have

$$p_{t1n} = \left( \frac{p_{t1}}{p_1} \right)_n p_1 = \left( \frac{1}{0.3187} \right) (20) = 62.8 \text{ psia}$$

$$p_{t2n} = \left( \frac{p_{t2}}{p_2} \right)_n p_2 = \left( \frac{1}{0.6925} \right) (41.7) = 60.2 \text{ psia}$$

We now proceed to calculate the stagnation temperatures and show that for the actual oblique-shock problem,  $T_t = 1515^\circ\text{R}$ , and for the normal-shock problem,  $T_t = 1386^\circ\text{R}$ . All of these static and stagnation pressures and temperatures are shown in the  $T-s$  diagram of Figure E7.4. This clearly shows the effect of superimposing the tangential velocity on top of the normal-shock problem with the corresponding change in stagnation reference. It is interesting to note that the *ratio* of stagnation pressures is the same whether figured from the oblique-shock problem or the normal-shock problem.

$$\frac{p_{t2}}{p_{t1}} = \frac{82.2}{85.7} = 0.959 \quad \frac{p_{t2n}}{p_{t1n}} = \frac{60.2}{62.8} = 0.959$$

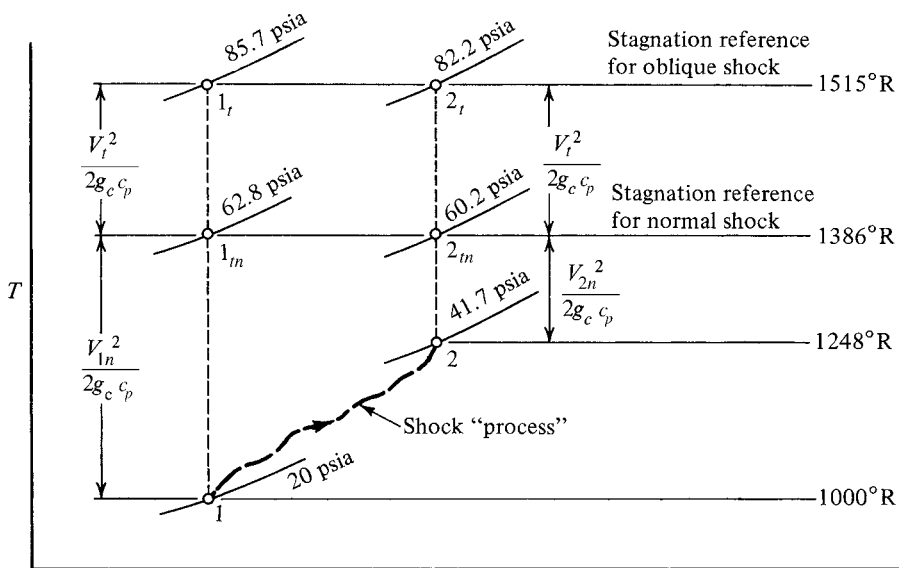


**Figure E7.4**  $T-s$  diagram for oblique shock (showing the included normal shock).

Is this a coincidence? No! Remember that the stagnation pressure *ratio* is a measure of the loss across the shock. Superposition of a tangential velocity onto a normal shock does not affect the actual shock process, so the losses remain the same. Thus, although one cannot use the stagnation pressures from the normal-shock problem, one can use the stagnation pressure *ratio* (which is listed in the tables). Be careful! These conclusions do *not* apply to the moving normal shock, which was discussed in Section 7.3.

## 7.5 OBLIQUE-SHOCK ANALYSIS: PERFECT GAS

In Section 7.4 we saw how an oblique shock could be viewed as a combination of a normal shock and a tangential velocity. If the initial conditions *and the shock angle* are known, the problem can be solved through careful application of the normal-shock table. Frequently, however, the shock angle is *not* known and thus we seek a new approach to the problem. The oblique shock with its components and angles is shown again in Figure 7.8.

Our objective will be to relate the deflection angle ( $\delta$ ) to the shock angle ( $\theta$ ) and the entering Mach number. We start by applying the continuity equation to a unit area at the shock:

$$\rho_1 V_{1n} = \rho_2 V_{2n} \quad (7.9)$$

or

$$\frac{\rho_2}{\rho_1} = \frac{V_{1n}}{V_{2n}} \quad (7.10)$$

From Figure 7.8 we see that

$$V_{1n} = V_1 \tan \theta \quad \text{and} \quad V_{2n} = V_2 \tan(\theta - \delta) \quad (7.11)$$

Thus, from equations (7.10) and (7.11),

$$\frac{\rho_2}{\rho_1} = \frac{V_{1n}}{V_{2n}} = \frac{V_1 \tan \theta}{V_2 \tan(\theta - \delta)} = \frac{\tan \theta}{\tan(\theta - \delta)} \quad (7.12)$$

From the normal-shock relations that we derived in Chapter 6, property ratios across the shock were developed as a function of the approaching (normal) Mach number. Specifically, the density ratio was given in equation (6.26) as

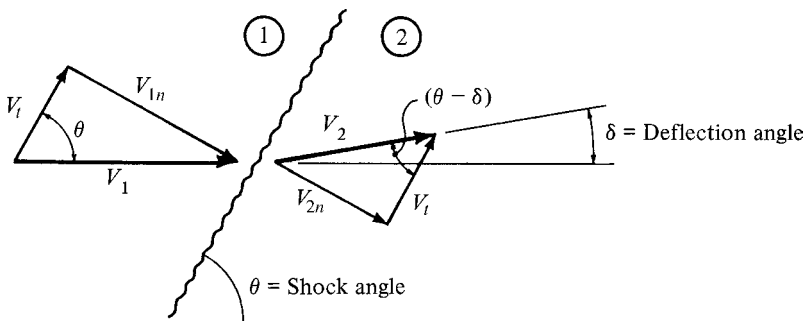


Figure 7.8 Oblique shock.

$$\frac{\rho_2}{\rho_1} = \frac{(\gamma + 1)M_{1n}^2}{(\gamma - 1)M_{1n}^2 + 2} \quad (6.26)$$

Note that we have added subscripts to the Mach numbers to indicate that these are normal to the shock. Equating (7.12) and (6.26) yields

$$\frac{\tan \theta}{\tan(\theta - \delta)} = \frac{(\gamma + 1)M_{1n}^2}{(\gamma - 1)M_{1n}^2 + 2} \quad (7.13)$$

But

$$M_{1n} = M_1 \sin \theta \quad (7.5)$$

Hence

$$\frac{\tan \theta}{\tan(\theta - \delta)} = \frac{(\gamma + 1)M_1^2 \sin^2 \theta}{(\gamma - 1)M_1^2 \sin^2 \theta + 2} \quad (7.14)$$

and we have succeeded in relating the shock angle, deflection angle, and entering Mach number. Unfortunately, equation (7.14) cannot be solved for  $\theta$  as an explicit function of  $M$ ,  $\delta$ , and  $\gamma$ , but we can obtain an explicit solution for

$$\delta = f(M, \theta, \gamma)$$

which is

$$\tan \delta = 2(\cot \theta) \left( \frac{M_1^2 \sin^2 \theta - 1}{M_1^2(\gamma + \cos 2\theta) + 2} \right) \quad (7.15)$$

It is interesting to examine equation (7.15) for the extreme values of  $\theta$  that might accompany any given Mach number.

For  $\theta = \theta_{\max} = \pi/2$ , equation (7.15) yields  $\tan \delta = 0$ , or  $\delta = 0$ , which we know to be true for the normal shock.

For  $\theta = \theta_{\min} = \sin^{-1}(1/M_1)$ , equation (7.15) again yields  $\tan \delta = 0$  or  $\delta = 0$ , which we know to be true for the limiting case of the Mach wave or no shock. Thus the relationship developed for the oblique shock includes as special cases the strongest shock possible (normal shock) and the weakest shock possible (no shock) as well as all other intermediate-strength shocks. Note that for the given deflection angle of  $\delta = 0^\circ$ , there are two possible shock angles for any given Mach number. In the next section we see that this holds true for any deflection angle.

## 7.6 OBLIQUE-SHOCK TABLE AND CHARTS

Equation (7.14) provides a relationship among the shock angle, deflection angle, and entering Mach number. Our motivation to obtain this relationship was to solve problems in which the shock angle ( $\theta$ ) is the unknown, but we found that an explicit solution  $\theta = f(M, \delta, \gamma)$  was not possible. The next best thing is to plot equation (7.14) or (7.15). This can be done in several ways, but it is perhaps most instructive to look at a plot of shock angle ( $\theta$ ) versus entering Mach number ( $M_1$ ) for various deflection angles ( $\delta$ ). This is shown in Figure 7.9.

One can quickly visualize from the figure all possible shocks for any entering Mach number. For example, the dashed vertical line at any arbitrary Mach number starts at the top of the plot with the normal shock ( $\theta = 90^\circ$ ,  $\delta = 0^\circ$ ), which is the strongest possible shock. As we move downward, the shock angle decreases continually to  $\theta_{\min} = \mu$  (Mach angle), which means that the shock strength is decreasing continually. Why is this so? What is the *normal Mach number* doing as we move down this line?

It is interesting to note that as the shock angle decreases, the deflection angle at first increases from  $\delta = 0$  to  $\delta = \delta_{\max}$ , and then the deflection angle decreases back to zero. Thus for any given Mach number and deflection angle, two shock situations are possible (assuming that  $\delta < \delta_{\max}$ ). Two such points are labeled A and B. One of these (A) is associated with a higher shock angle and thus has a higher normal Mach number, which means that it is a stronger shock with a resulting higher pressure ratio. The other (B) has a lower shock angle and thus is a weaker shock with a lower pressure rise across the shock.

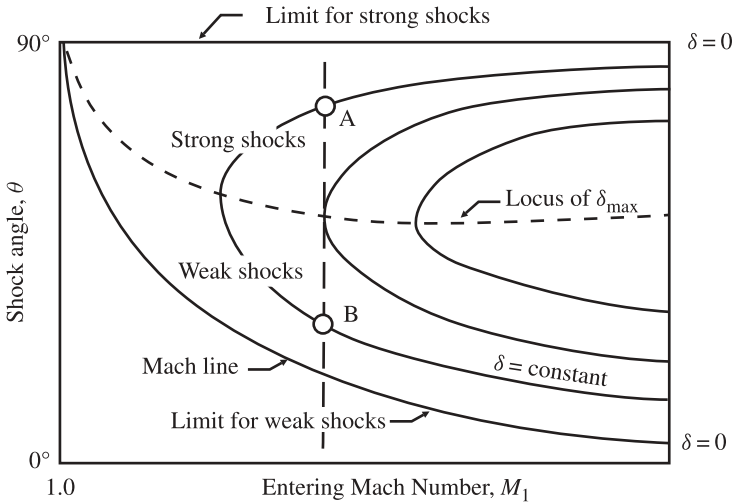


**Figure 7.9** Skeletal oblique shock relations among  $\theta$ ,  $M_1$ , and  $\delta$ . (See Appendix D for detailed working charts.)

All of the *strong shocks* (above the  $\delta_{\max}$  points) result in *subsonic flow* after passage through the shock wave. In general, nearly all the region of *weak shocks* (below  $\delta_{\max}$ ) result in *supersonic flow* after the shock, although there is a very small region just below  $\delta_{\max}$  where  $M_2$  is still subsonic. This is clearly shown on the *detailed working chart* in Appendix D. Normally, we find the weak shock solution occurring more frequently, although this is entirely dependent on the boundary conditions that are imposed. This point, along with several applications of oblique shocks, is the subject of the next two sections. In many problems, explicit knowledge of the shock angle  $\theta$  is not necessary. In Appendix D you will find two additional charts which may be helpful. The first of these depicts the Mach number after the oblique shock  $M_2$  as a function of  $M_1$  and  $\delta$ . The second shows the static pressure ratio across the shock  $p_2/p_1$  as a function of  $M_1$  and  $\delta$ . One can also use detailed oblique-shock tables such as those by Keenan and Kaye (Ref. 31). Another possibility is to use equation (7.15) with a computer as discussed in Section 7.10. Use of the table or of equation (7.15) yields higher accuracies, which are essential for some problems.

**Example 7.5** Observation of an oblique shock in air (Figure E7.5) reveals that a Mach 2.2 flow at 550 K and 2 bar abs. is deflected by  $14^\circ$ . What are the conditions after the shock? Assume that the weak solution prevails.

We enter the chart (in Appendix D) with  $M_1 = 2.2$  and  $\delta = 14^\circ$  and we find that  $\theta = 40^\circ$  and  $83^\circ$ . Knowing that the weak solution exists, we select  $\theta = 40^\circ$ .

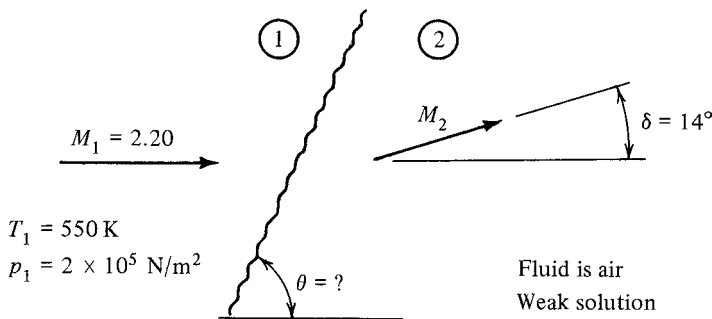


Figure E7.5

$$M_{1n} = M_1 \sin \theta = 2.2 \sin 40^\circ = 1.414$$

Enter the normal-shock table at  $M_{1n} = 1.414$  and interpolate:

$$M_{2n} = 0.7339 \quad \frac{T_2}{T_1} = 1.2638 \quad \frac{p_2}{p_1} = 2.1660$$

$$T_2 = \frac{T_2}{T_1} T_1 = (1.2638)(550) = 695 \text{ K}$$

$$p_2 = \frac{p_2}{p_1} p_1 = (2.166)(2 \times 10^5) = 4.33 \times 10^5 \text{ N/m}^2$$

$$M_2 = \frac{M_{2n}}{\sin(\theta - \delta)} = \frac{0.7339}{\sin(40 - 14)} = 1.674$$

We could have found  $M_2$  and  $p_2$  using the other charts in Appendix D. From these the value of  $M_2 \approx 1.5$  and  $p_2$  is found as

$$p_2 = \frac{p_2}{p_1} p_1 \approx (2)(2 \times 10^5) = 4 \times 10^5 \text{ N/m}^2$$

## 7.7 BOUNDARY CONDITION OF FLOW DIRECTION

We have seen that one of the characteristics of an oblique shock is that the flow direction is changed. In fact, this is *one of only two methods* by which a supersonic flow can be turned. (The other method is discussed in Chapter 8.) Consider supersonic flow over a wedge-shaped object as shown in Figure 7.10. For example, this could represent the leading edge of a supersonic airfoil. In this case the flow is forced to change direction to *meet the boundary condition of flow tangency along the wall*, and this can be done only through the mechanism of an oblique shock. The example in Section 7.6 was just such a situation. (Recall that a flow of  $M = 2.2$  was deflected by  $14^\circ$ .) Now, for any given Mach number and deflection angle there are two possible shock angles. Thus a question naturally arises as to which solution will occur, the *strong* one or the *weak* one. Here is where the surrounding pressure must be considered. Recall that the strong shock occurs at the higher shock angle and results in a large pressure change. For this solution to occur, a physical situation must exist that can sustain the necessary pressure differential. It is conceivable that such a case might exist in an *internal* flow situation. However, for an *external* flow situation such as around the

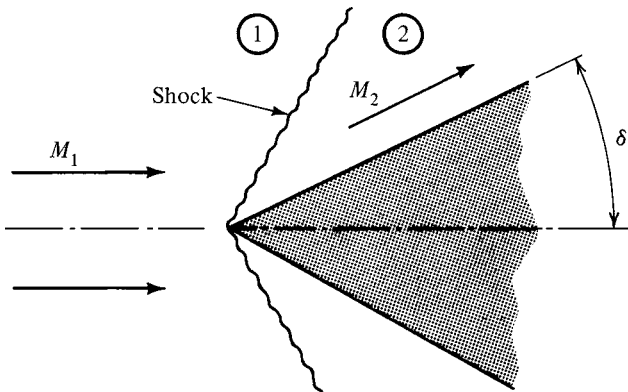


Figure 7.10 Supersonic flow over a wedge.

airfoil, there is no means available to support the greater pressure difference required by the strong shock. Thus, in external flow problems (flow around objects), we always find the weak solution.

Looking back at Figure 7.9 you may notice that there is a maximum deflection angle ( $\delta_{\max}$ ) associated with any given Mach number. Does this mean that the flow cannot turn through an angle greater than this? This is true if we limit ourselves to the simple oblique shock that is *attached* to the object as shown in Figure 7.10. But what happens if we build a wedge with a half angle greater than  $\delta_{\max}$ ? Or suppose we ask the flow to pass over a blunt object? The resulting flow pattern is shown in Figure 7.11.

A *detached shock* forms which has a curved wave front. Behind this wave we find all possible shock solutions associated with the initial Mach number  $M_1$ . At the center a normal shock exists, with subsonic flow resulting. Subsonic flow has no difficulty adjusting to the large deflection angle required. As the wave front curves around, the shock angle decreases continually, with a resultant decrease in shock strength. Eventually, we reach a point where supersonic flow exists after the shock front. Although Figures 7.10 and 7.11 illustrate flow over objects, the same patterns result from internal flow along a wall, or *corner flow*, shown in Figure 7.12. The significance of  $\delta_{\max}$  is again seen to be the maximum deflection angle for which the shock can remain *attached* to the corner.

A very practical situation involving a detached shock is caused when a pitot tube is installed in a supersonic tunnel (see Figure 7.13). The tube will reflect the total pressure after the shock front, which at this location is a normal shock. An additional

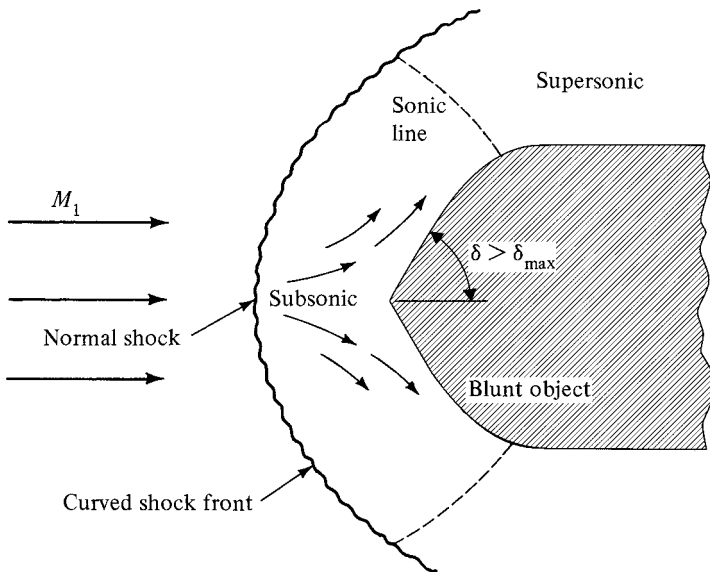


**Figure 7.11** Detached shock caused by  $\delta > \delta_{\max}$ .

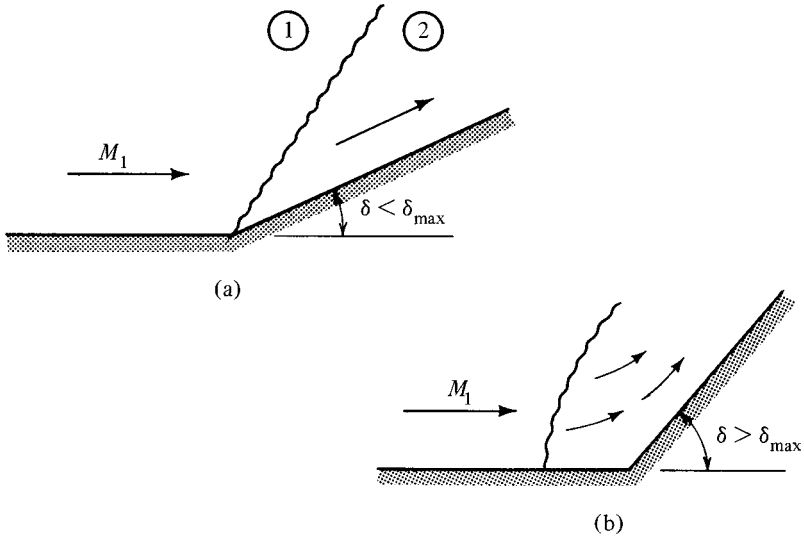


Figure 7.12 Supersonic flow in a corner.

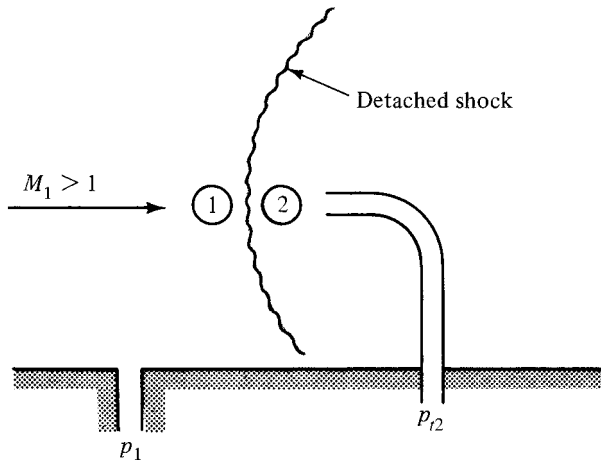


Figure 7.13 Supersonic pitot tube installation.

tap off the side of the tunnel can pick up the static pressure ahead of the shock. Consider the ratio

$$\frac{p_{t2}}{p_1} = \frac{p_{t2}}{p_{t1}} \frac{p_{t1}}{p_1}$$

$p_{t2}/p_{t1}$  is the total pressure ratio across the shock and is a function of  $M_1$  only [see equation (6.28)].  $p_{t1}/p_1$  is also a function of  $M_1$  only [see equation (5.40)]. Thus the

ratio  $p_{t2}/p_1$  is a function of the initial Mach number and can be found as a parameter in the shock table.

**Example 7.6** A supersonic pitot tube indicates a total pressure of 30 psig and a static pressure of zero gage. Determine the free-stream velocity if the temperature of the air is 450°R.

$$\frac{p_{t2}}{p_1} = \frac{30 + 14.7}{0 + 14.7} = \frac{44.7}{14.7} = 3.041$$

From the shock table we find that  $M_1 = 1.398$ .

$$a_1 = [(1.4)(32.2)(53.3)(450)]^{1/2} = 1040 \text{ ft/sec}$$

$$V_1 = M_1 a_1 = (1.398)(1040) = 1454 \text{ ft/sec}$$

So far we have discussed oblique shocks that are caused by flow deflections. Another case of this is found in engine inlets of supersonic aircraft. Figure 7.14 shows a sketch of an aircraft that is an excellent example of this situation. As aircraft and missile speeds increase, we usually see two directional changes with their accompanying shock systems, as shown in Figure 7.15. The losses that occur across the

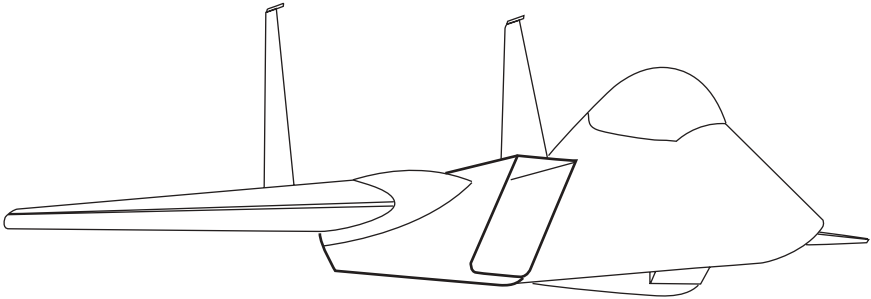


**Figure 7.14** Sketch of a rectangular engine inlet.

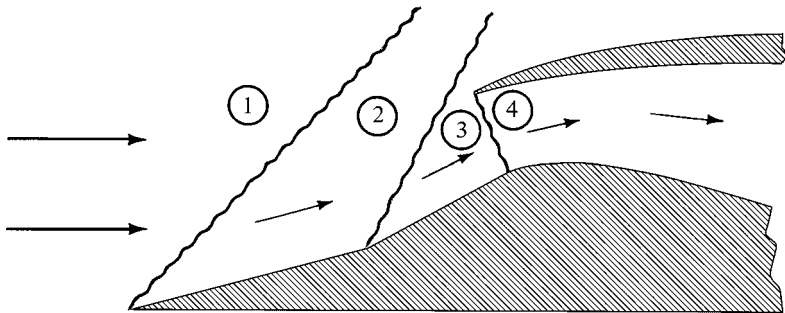


**Figure 7.15** Multiple-shock inlet for supersonic aircraft.

series of shocks shown are less than those which would occur across a single normal shock at the same initial Mach number. A warning should be given here concerning the application of our results to inlets with circular cross sections. These will have conical *spikes* for flow deflection which cause *conical-shock* fronts to form. This type of shock has been analyzed and is covered in Section 7.9. The design of supersonic diffusers for propulsion systems is discussed further in Chapter 12.

In problems such as the multiple-shock inlet and the supersonic airfoil, we are generally not interested in the shock angle itself but are concerned with the resulting Mach numbers and pressures downstream of the oblique shock. Remember that the charts in Appendix D show these exact variables as a function of  $M_1$  and the turning angle  $\delta$ . The stagnation pressure ratio can be inferred from these using the proper relations.

## 7.8 BOUNDARY CONDITION OF PRESSURE EQUILIBRIUM

Now let us consider a case where the existing pressure conditions cause an oblique shock to form. Recall our friend the converging–diverging nozzle. When it is operating at its second critical point, a normal shock is located at the exit plane. The pressure rise that occurs across this shock is exactly that which is required to go from the low pressure that exists within the nozzle up to the higher receiver pressure that has been imposed on the system. We again emphasize that *the existing operating pressure ratio is what causes the shock to be located at this particular position*. (If you have forgotten these details, review Section 6.6.)

We now ask: What happens when the operating pressure ratio is between the second and third critical points? A normal shock is too strong to meet the required pressure rise. What is needed is a compression process that is weaker than a normal shock, and our oblique shock is precisely the mechanism for the job. *No matter what pressure rise is required*, the shock can form at an angle that will produce any desired pressure rise from that of a normal shock on down to the third critical condition, which requires no pressure change. Figure 7.16 shows a typical weak oblique shock at the

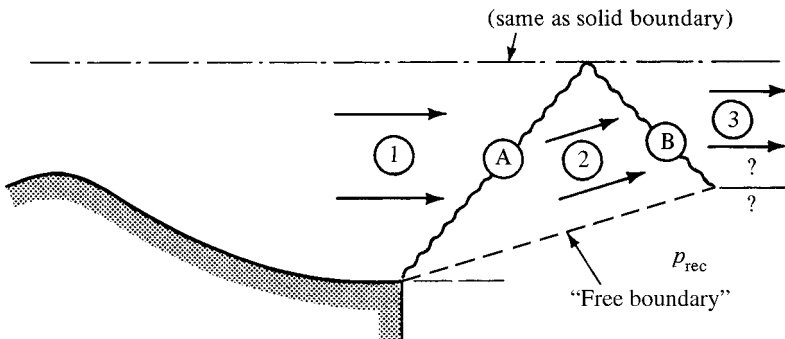


**Figure 7.16** Supersonic nozzle operating between second and third critical points.